Unbound states by analytic continuation in the coupling constant

N. Tanaka,[1] Y. Suzuki,[2] K. Varga,[3,4] and R. G. Lovas[3]
[1]*Graduate School of Science and Technology, Niigata University, Niigata 950-2181, Japan*
[2]*Department of Physics, Niigata University, Niigata 950-2181, Japan*
[3]*Institute of Nuclear Research of the Hungarian Academy of Sciences, P. O. Box 51, H-4001 Debrecen, Hungary*
[4]*Physics Division, Argonne National Laboratory, 9700 South Cass Avenue, Argonne, Illinois 60439*
(Received 20 July 1998)

The energies and widths of resonance states are determined by the analytic continuation of bound-state energies as functions of a potential strength parameter (''the coupling constant''). Various numerical examples show the applicability of the method to systems decaying to two- and three-body channels. The examples include unbound states of the nuclei ^{5}He, ^{5}Li, ^{9}Be, and ^{9}B, described in $\alpha+N$ and $\alpha+\alpha+N$ microscopic cluster models. Some states considered are controversial. Here they are well defined, and their questionable features are understood to arise from their proximity to the complex-energy region of unphysical resonances with negative energies and positive widths. [S0556-2813(99)00103-X]

PACS number(s): 25.70.Ef, 21.60.Gx, 27.10.+h, 27.20.+n

I. INTRODUCTION

In addition to bound states, nuclei have a large number of discrete unbound states [1]. In standard nuclear structure models square-integrable bases are used, disregarding thresholds and the decay of some states. The instability of a state is often essential. Neglecting it may lead to false conclusions about other properties as well. The problem is especially acute for light nuclei, which often have just one bound state or none. Without consideration of unbound states or disregarding their instability, the description is incomplete and unreliable.

In recent years, however, new phenomena discovered in the field of unstable nuclei have revived the interest in unbound states. One of the most prominent phenomena is the ''Borromean'' binding [2]. A system is called Borromean if it is bound but can be decomposed into three subsystems, any two of which cannot form a bound state. Examples are the nuclei ^{6}He and ^{11}Li, composed of $\alpha+n+n$ and ^{9}Li $+n+n$, respectively.

Unbound states may be put on the same footing as bound states by the concept of the *S*-matrix pole (see, e.g., [3,4]). The pole position in different regions of the complex plane is used to characterize the unbound states (resonances, ''virtual states,'' etc.). The techniques to find the poles of the *S* matrix have been mostly limited to simple interactions and systems. For composite nuclear systems one should treat the structure and the instability simultaneously. Although there exist methods designed for resonance states (see, e.g., Refs. [5,6]), it is desirable to deduce the properties of unbound states from the eigenvalues and eigenfunctions of suitable Hamiltonians. For that purpose computational methods developed for bound states can be used effectively. Two methods of this type are widely used in atomic and nuclear physics. In the first method, called the real stabilization method [7], the Schrödinger equation is solved in a box and the resonances are singled out from the continuum by exploiting their stability against changes of the box size. In this method one has to solve the Schrödinger equation with many different box sizes, and with the many-dimensional box to contain a multiparticle system, it is sometimes difficult to find the appropriate box sizes. The method turns out to be suitable for narrow resonances only. In the second method, called the complex scaling method (CSM) [8], the coordinate $\mathbf{r}$ is rotated into the complex plane by the transformation $\mathbf{r}\rightarrow e^{i\theta}\mathbf{r}$, which transforms the resonance wave function into a square-integrable function, while leaving the pole position intact. The CSM involves the calculation of complex matrix elements and the solution of a complex eigenvalue problem. Its main difficulty is that the Hamiltonian is non-Hermitian, and the variational method used does not give an energy minimum. Thus it becomes cumbersome to optimize the bases. The CSM has nevertheless proved to be suitable for exploring resonances, but not virtual states.

A third bound-state-type method [9] is that of the analytic continuation in a coupling constant (ACCC). This approach draws on the intuitive picture that unbound states can be related to bound states by continuation to weaker binding. More precisely, the unbound-state problem is first transformed into a bound-state problem by artificially changing a strength parameter in the potential. Then the square root of the bound-state energy is continued analytically as a function of the strength parameter to complex values by a Padé approximant. The coefficients of the Padé approximant are determined by the real eigenvalues of the Hamiltonian for several different potential strengths. Matrix elements of the Hamiltonian are real and need not be calculated repeatedly, contrary to the real stabilization method or the CSM.

The ACCC method has hitherto been applied only in a few simple test cases owing probably to the high accuracy required of the solution of the bound-state problem by the Padé approximation. The emergence of reliable methods to solve few-body problems has, however, widened the applicability of the ACCC method. In our previous paper [10] we tested the ACCC method by comparing its performance with those of the direct numerical integration (DNI) and of the CSM. The examples included both two-body and three-body resonances. The satisfactory agreement found in these cases demonstrates that the ACCC method provides an effective description of nuclear resonances.

The purpose of this paper is to apply the ACCC method to some specific unbound states, which test the analytic continuation technique. One is an *S*-wave resonance or a virtual state, whose trajectory near threshold shows a behavior quite different from resonances in other partial waves. We will also consider three-body systems, which accommodate both well-behaved resonance states and irregular ones.

The three-body systems to be considered are the Borromean systems $^9\mathrm{Be}=\alpha+\alpha+n$ and $^9\mathrm{B}=\alpha+\alpha+p$, and the two-body systems to be considered are their subsystems $^5\mathrm{He}=\alpha+n$ and $^5\mathrm{Li}=\alpha+p$. They will be described microscopically, i.e., as nine- and five-nucleon systems, respectively. The terms ''three-body'' and ''two-body'' refer to the number of clusters we consider. The structure of the nuclei ^{9}Be and ^{9}B was recently investigated in a microscopic three-cluster model by Arai, Ogawa, and two of the present authors (Y.S. and K.V.) [11]. They applied the CSM method and found all low-lying resonances except the $1/2^+$ states. The $1/2^+$ state of ^{9}Be, known to have an enhanced electric dipole transition to the ground state, has an energy of 110 keV above the $\alpha+\alpha+n$ threshold and a width of about 220 keV [12]. Its analog state in ^{9}B is also of considerable interest (see, e.g., Refs. [13–15]), but its energy has not yet been determined experimentally. The ACCC method offers the possibility to study these states.

In Sec. II we outline the ACCC method. As an illustration, a simple two-body model will be discussed. Some resonances of ^{5}He and ^{5}Li will be examined in the microscopic two-cluster models of $\alpha+n$ and $\alpha+p$. Section III is devoted to three-body systems, and as an application, a few resonances of ^{9}Be and ^{9}B will be discussed, with particular emphasis on the $1/2^+$ states. Some conclusions are drawn in Sec. IV.

II. ANALYTIC CONTINUATION IN COUPLING CONSTANTS

A. Poles of the *S* matrix: A simple example

We assume that the Hamiltonian of the system is written as $H(\lambda)=H_1+\lambda H_2$, where H_2 is an attractive interaction such that H has a bound state for some values of λ. When λ is decreased the bound state approaches threshold and may become a resonance or a virtual state. The value of λ for which $E(\lambda)=0$ will be denoted by λ_0.

The *S*-matrix formulation provides a unified description of discrete and continuum states. The discrete states are associated with the poles of the scattering matrix $S_l(k)$, where l is the orbital angular momentum. The matrix $S_l(k)$, defined originally for positive real wave number k, can be continued analytically to the complex k plane. As is well known [3,4], the poles on the positive imaginary k axis belong to bound states, while the poles on the negative imaginary axis also imply negative energies, but the corresponding wave functions diverge exponentially at large distances. Such ''states'' are called virtual or antibound states. If a pole is located in the fourth quadrant of the complex k plane, i.e.,

$$k=k_R-ik_I, \quad k_R>0, \quad k_I>0, \tag{1}$$

then its complex energy is $E=\hbar^2k^2/2m\equiv E_R-i\Gamma/2$, where

$$E_R=\frac{\hbar^2}{2m}(k_R^2-k_I^2), \quad \Gamma=\frac{2\hbar^2}{m}k_Rk_I>0. \tag{2}$$

If $k_R>k_I$, then $E_R>0$ and the pole corresponds to an exponentially decaying state or ''resonance,'' with position E_R and width Γ. This will only give rise to a resonant structure in $S_l(k)$ for real momenta if Γ is sufficiently small. If $k_R<k_I$, then the real part of the energy becomes negative, and the ''resonance'' is said to be ''unphysical.'' The *S* matrix will also have another pole at $k=-k_R-ik_I$ in the third quadrant, which corresponds to a quasistationary state, which is associated with capture, and it is sometimes called an antiresonance.

The above discussion can be illustrated with a square well potential $[H_1=\mathbf{p}^2/2m, H_2=V(r), \quad V(r)=-\lambda V_0 (r<a), \; V(r)=0 (r\geq a)]$. The Schrödinger equation then can be solved analytically, which makes it possible to locate the *S*-matrix poles easily. The upper panel of Fig. 1 displays some of the poles for $l=0$ and 1 for a square well potential. The parameters are the same as used in Refs. [16,1]: $\hbar^2/2m=4$ MeV fm^2, $a=2$ fm, $\lambda=1$, and $V_0=25$ MeV for $l=0$ and 12.25 MeV for $l=1$. There are two bound states and one virtual state in the *S* wave and one bound state and one virtual state in the *P* wave. There are, in addition, some poles located in the third and fourth quadrants of the complex k plane. The middle panel of Fig. 1 displays the trajectories of the poles corresponding to the second bound state and to the virtual state in the *S* wave and that belonging to the *P*-wave bound state, as the coupling constant λ is decreased. By decreasing λ, the *S*-wave bound-state and virtual-state poles approach each other along the imaginary axis and merge at $\beta=ka=-i$. By further decreasing λ, the poles move, symmetrically, perpendicular to the imaginary axis into the fourth and third quadrants, respectively. The 1*S* pole represents a bound state for $0.890<\lambda\leq 1$. It represents a virtual state or an unphysical resonance for $0.804<\lambda\leq 0.890$ and corresponds to a resonance for $\lambda\leq 0.804$. The non-*S*-wave poles behave differently. The bound-state *P*-wave pole meets its virtual-state partner at the origin, and both leave the origin, symmetrically with respect to the imaginary axis and tangentially with respect to the real axis. One of the poles corresponds to a resonance for $0.110<\lambda\leq 0.806$, but by further decreasing λ, it enters the unphysical region. The lowest panel shows the real parts of the 1*S* and 0 *P* energies (E_R) as functions of λ. The two curves behave very differently near threshold. By decreasing λ, the *S*-state energy touches the $E_R=0$ axis, and turns negative again—reflecting the fact that the pole moves, through the origin, to the negative imaginary k axis—and it shows a kink where Rek becomes nonzero. On the other hand, the passage of the *P*-wave state through the threshold is smooth.

B. Analytic continuation of the square root of the energy

In Refs. [9,1] it has been shown that, for a two-body system interacting with an attractive short-range potential, the wave number k_l behaves near the threshold as $k_l(\lambda)\sim i\sqrt{\lambda-\lambda_0}$ for $l>0$ and $k_0(\lambda)\sim i(\lambda-\lambda_0)$ for $l=0$. It is thus convenient to introduce the variable

$$x=\sqrt{\lambda-\lambda_0}, \quad \text{with} \quad k_l(\lambda_0)=0, \tag{3}$$

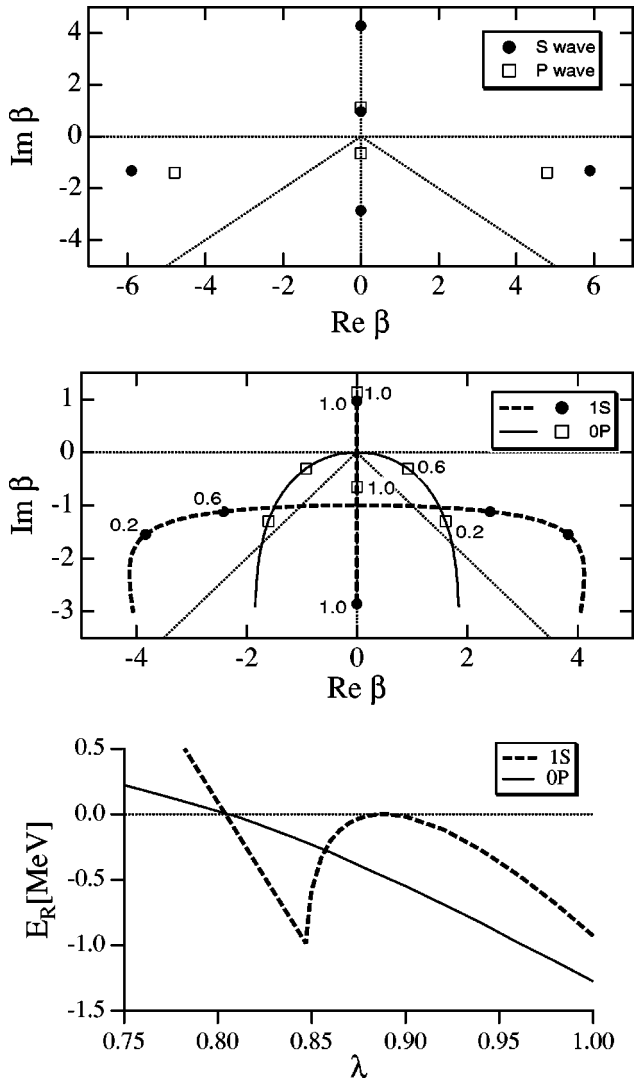

FIG. 1. S-matrix poles in a square well potential of radius a and depth $-\lambda V_0$. Uppermost panel: S- and P-wave poles in the complex $\beta=ka$ plane, where k is the wave number; $\lambda=1$. The dotted lines mark Im $\beta=\pm\mathrm{Re}\beta$. Middle panel: S- and P-wave pole trajectories in the β plane, with some λ values displayed. The dotted line as above. Lowest panel: (real parts of) the energies of the $1S$ and $0P$ states as a function of λ.

and continue $k_l(x)$, which is an analytic function in the bound-state region $\lambda>\lambda_0$, to the unbound region $\lambda<\lambda_0$. The threshold behavior of $k_l(x)$ allows one to perform the analytic continuation with a Padé approximant of the form

$$k_l(x)=i\frac{c_0+c_1x+c_2x^2+\cdots+c_Mx^M}{1+d_1x+d_2x^2+\cdots+d_Nx^N}. \tag{4}$$

For the S-wave pole, however, more careful considerations are necessary. As shown in Fig. 1 the sharp off-turn of the pole trajectory from the imaginary k axis (with the coincidence of the two poles) takes place below zero at a certain $-i\bar{\kappa}_0(\bar{\kappa}_0\geqslant 0)$, with the behavior at the kink similar to that for $l>0$:

$$k_0(\lambda)+i\bar{\kappa}_0\sim i\sqrt{\lambda-\bar{\lambda}_0}\quad\text{for}\quad\lambda\approx\bar{\lambda}_0, \tag{5}$$

where $\bar{\lambda}_0$ is defined by $k_0(\bar{\lambda}_0)=-i\bar{\kappa}_0$. Since the continuation is problematic at the kink, the variable x should be chosen to be zero at the kink. The definition of x in Eq. (4) is therefore replaced by

$$x=\sqrt{\lambda-\bar{\lambda}_0}\quad\text{with}\quad k_0(\bar{\lambda}_0)=-i\bar{\kappa}_0. \tag{6}$$

The $(M+N+1)$ coefficients of the $[N,M]$ Padé approximant (4) are calculated in the bound-state region and they are therefore real. If $\lambda<\lambda_0$ (or $\bar{\lambda}_0$), then x will be imaginary and $k_l(x)$ may become complex. To determine the coefficients c_i and d_i, we solve the bound-state problem for various values of the coupling constant $\lambda(>\lambda_0)$ and try to find the threshold value λ_0 or the kink value $\bar{\lambda}_0$. To have a reliable approximation, one has to know the c_i and d_i values accurately, and for that, one has to solve the bound-state problem to high accuracy (typically four or more digits), especially near the threshold. To solve the bound-state problem, we use the stochastic variational method with correlated Gaussian bases [17,18]. A point to be emphasized here is that one must accurately and consistently calculate a range of states with deep to weak binding up through the threshold, and that is a challenge for a variational calculation.

It was shown in Ref. [1] that both the $l=0$ and $l=1$ trajectories in Fig. 1 can be well reproduced by using the [5,5] Padé approximant. For S waves, $\bar{\lambda}_0$ is determined iteratively by searching for the value that produces the most stable trajectory, independently of the choice of the set of the bound-state energies which are used to determine the c_i and d_i values. If an incorrect value were used for $\bar{\lambda}_0$, then the trajectory would be very unstable and would strongly depend on the choice of the energy set as well as on the degree $[N,M]$ of the Padé approximant.

The threshold behavior of the pole trajectories shows to what extent the potential can confine a particle in an unbound state, and that, in turn, depends primarily on the penetrability of its surface. It is well known that there is no proper resonance without a barrier. To elucidate the dependence of the threshold behavior on barrier penetrability, we use a two-particle model with a two-range Gaussian potential

$$V(r)=-8\lambda\exp\{-(r/2.5)^2\}+B\exp\{-(r/5)^2\}, \tag{7}$$

where we use units of $\hbar=c=m=1$ (m is the particle mass). The second term produces a potential barrier. This simple problem can easily be solved by DNI [19]. The trajectories of the S-wave resonances obtained by the ACCC method and by DNI are compared in Fig. 2 for five barrier heights B (including $B=0$). We see that the trajectories for $B=1.0$ and 2.0 leave the imaginary k axis near the origin (i.e., $\bar{\kappa}_0\approx 0$), entering almost immediately the resonance region in a way reminiscent of the trajectories of higher partial waves. The trajectory passes fairly close to the real axis, implying small resonance widths. As the barrier height decreases, the trajectory tends to be similar to that of an S-wave pole in the purely attractive potential (Fig. 1): it follows the negative imaginary axis for a while, and the corresponding state is virtual; then it leaves the axis at a certain point ($\bar{\kappa}_0>0$) into the unphysical region before it enters the resonance region.

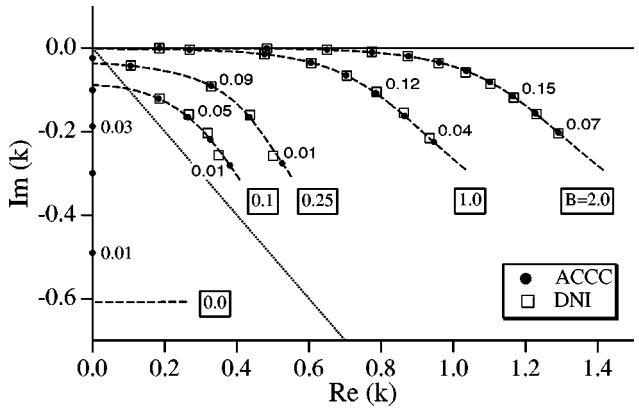

FIG. 2. Pole trajectories in the two-range Gaussian potential of Eq. (7). ACCC results are compared with DNI results. The trajectories are obtained by varying λ, and the points marked belong to equidistant λ. The dotted line marks Im $k=-\mathrm{Re}k$.

C. Application to ^{5}He and ^{5}Li

As an application of the ACCC method to a two-body system, we calculate the resonance parameters of ^{5}He and ^{5}Li. These have been determined by *R*-matrix analyses (see, e.g., [20]) and have also been calculated by a microscopic cluster model [the resonating-group model (RGM); see, e.g., [21]]. The $3/2^-$ and $1/2^-$ resonances have been identified experimentally [12], though the width of the latter is very large and its energy is uncertain. The existence of a $1/2^+$ resonance is even more controversial [22]. A recent shell-model calculation [23] puts it at 3–4 MeV for ^{5}He. If the state were predominantly of single-particle nature as is found in Ref. [23], its existence would be a great surprise.

We assume that the resonances in the $A=5$ systems have the two-cluster structure of $\alpha+N$. The wave function of the α particle, Φ_α, is approximated by a $(0s)^4$ harmonic-oscillator configuration (the center-of-mass motion eliminated) with size parameter $\nu\equiv m\omega/2\hbar=0.26$ fm^{-2}. It is too difficult to use a more sophisticated wave function, especially in three-cluster model calculations. The trial wave function is then given by

$$\Psi=\mathcal{A}\{\Phi_\alpha F(r)[Y_l(\hat{\mathbf{r}})\times\chi_{1/2}]_{JM}\}, \tag{8}$$

where $\mathcal{A}$ is the antisymmetrizer and $\chi_{1/2}$ is the spin function of the nucleon. Our model is rather similar to that used in [21]. The radial α-N relative wave function $F(r)$ is determined variationally by minimizing the energy. It was expressed as a combination of Gaussians with different falloff parameters. Since the wave function of the α particle is approximated by the simplest shell-model configuration, we have to use such an effective two-nucleon potential that reproduces reasonably well the binding energy of the α particle with that configuration as well as two-nucleon scattering data at low energies. As such a potential we used the Minnesota two-nucleon potential [24]. Its central term contains an exchange parameter u, which determines the potential strength in odd partial waves. The appropriate u value $\bar{u}$ depends somewhat on the system. Since the energy of the only composite subsystem, the α particle, does not depend on u, it is convenient to choose $\lambda=u/\bar{u}$, but for simplicity, we considered u itself as the variable. To facilitate the analytic continuation, the bound-state calculation was performed for a set of u values.

TABLE I. Resonance energies E and widths Γ, given in units of MeV, of ^{5}He and ^{5}Li. $\bar{u}=0.98$. The energy is counted from the two-body threshold.

		ACCC			*S* matrix, RGM [a]		Expt. [b]	
	J^π	E	Γ	u_0	E	Γ	E	Γ
^{5}He	$3/2^-$	0.77	0.64	1.10415	0.76	0.63	0.89	0.60
	$1/2^-$	1.98	5.4	1.6775	1.89	5.20	5 ± 1	4 ± 1
	$1/2^+$	12	190	2.2261				
^{5}Li	$3/2^-$	1.63	1.25	1.20588	1.67	1.33	1.97	≈1.5
	$1/2^-$	3.0	6.4	1.800653	2.70	6.25	$7-12$	5 ± 2
	$1/2^+$	42	197	2.428761				

[a]Reference [21].
[b]Reference [12].

Although the bound-state problem must be solved many times, the ACCC method does not require a large amount of computer time. Since the Hamiltonian is linear in the coupling constant, its matrix elements must be evaluated only once. The diagonalization of the Hamiltonian, which must be repeated many times, is not very time consuming.

The calculation was done for $J^\pi=3/2^-(l=1)$, $1/2^-(l=1)$, and $1/2^+(l=0)$. The resonance parameters predicted by the ACCC method for $\bar{u}=0.98$ are listed in Table I. The u values corresponding to the thresholds, u_0, are also listed in the table. Since u_0 is close to $\bar{u}=0.98$ for the $3/2^-$ state, the analytic continuation is very stable. For the $1/2^-$ state, the u_0 value is fairly far from $\bar{u}$, yet the analytic continuation involves little uncertainty.

The RGM results of [21] were obtained by performing scattering calculations for complex energies. Table I shows that our results are consistent with them. The two models are not exactly the same, and so small differences are natural. Whenever one energy is smaller than the other, the corresponding widths behave similarly, which indicates a consistent shift specific to each partial wave. The RGM of Ref. [21] reproduces the experimental phase shifts excellently, but the resonance parameters agree with the empirical parameters for only the $3/2^-$ states. The discrepancy in the position of the $1/2^-$ state is caused by the fact that the parameters of a broad resonance are poorly defined empirically. The unique definition is that based on the *S*-matrix pole, and if that definition is used in the analyses [25], there is no discrepancy.

More interesting is the $1/2^+$ state. Figure 3 displays the analytic continuation from the bound-state region by varying u. In this case the distance between the physical value, $\bar{u}=0.98$, and u_0 is extremely large and this makes the analytic continuation rather unstable. The trajectory for the ^{5}He system passes through the virtual-state region and the unphysical region of the fourth quadrant and finally shows up in the physical region before reaching $\bar{u}=0.98$. This trajectory is reminiscent of the *S*-wave trajectory in a potential problem of no barrier (see Fig. 2). The point $\bar{u}=0.98$ is very close to the borderline separating the physical region from the unphysical region. The energy of the state is therefore predicted

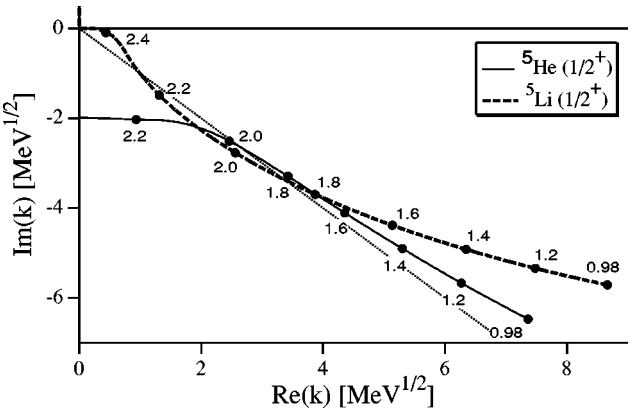

FIG. 3. The trajectories of the $1/2^+$ states in ^{5}He and ^{5}Li as a function of the u parameter. Here k is identified with $E^{1/2}$. The dotted line marks Im $k=-\mathrm{Re}k$.

to be much smaller than the width. Such a state does not show up in the phase shift, and so it cannot be called a proper resonance. The case of ^{5}Li is similar to that of ^{5}He, except that the trajectory resembles the pattern of the finite-barrier case of Fig. 2. Because of the instability of the analytic continuation, the $1/2^+$ resonance parameters in Table I are rather uncertain. Nevertheless, the shape of the trajectories is likely to be qualitatively correct; so the $1/2^+$ states must lie close to the borderline between physical and unphysical resonances. The present model could, of course, be improved, but that would not help since this model reproduces the experimental phase shifts, and so any improvement should be accompanied by a rescaling of the parameters. For example, the distortion of the α particle would increase the binding for all states. For the $A=6$ nuclei this effect is of the order of 1 MeV [26]. This is an overall shift, which has to be compensated for by a change of u to restore the agreement in other observables. Therefore, the resonance parameters produced by our model are very likely realistic. We thus think it is fair to say that our results rule out the existence of a low-lying $1/2^+$ resonance in ^{5}He and ^{5}Li.

III. RESONANCES IN THREE-BODY SYSTEMS

A. Resonance of a Borromean system

The resonances of three-body systems have physical significance in various problems. It is of great interest to see whether there are resonances in the three-nucleon system or in the three-baryon systems of ΛNN and ΣNN, and whether the so-called dibaryon resonance exists in the πNN system. The S-matrix pole trajectories have been studied for three-body systems interacting via schematic potentials [27–29]. In these works the Faddeev formalism was used for the three-body dynamics, and the S-matrix poles were obtained by analytic continuation of the solution of the eigenvalue equation of the Faddeev kernel. Recently, three-nucleon resonances were searched for by the CSM [30].

As our variational method provides extremely accurate bound-state solutions for three particles or even more [18,31], we can extend our studies to three-body systems. From the behavior of the two-body pole trajectories one cannot tell *a priori* whether the three-body trajectories behave in the same way. To conjecture their qualitative behavior, it would be convenient to think in terms of an ''effective'' two-body picture, but to set up such a picture is nontrivial. An example of a nontrivial three-body effect is the Efimov effect [32]: the three-body system will have an infinite number of bound states if none of the two-body subsystems has a bound state but all have S states sharp at zero energy. Thus one can expect that the behavior of the three-body state depends crucially on whether the subsystems have bound states or not.

The physical system we shall study is Borromean, with or without two-body (Coulomb) barriers. To get a feeling for the behavior of the trajectory in these cases, we now consider a simple Borromean system of three spinless bosons of mass m, with $\hbar^2/m=41.47$ MeV fm^2, which interact via the potential

$$V(r)=-80\lambda\,\exp\{-r^2\}+B\,\exp\{-(r/3)^2\}. \tag{9}$$

The energies and lengths are in units of MeV and fm, respectively. Note that there are no two-body bound states for $\lambda<1.5$. Thus, if there is a resonance at $\lambda=1$, it will decay into three-body channels. We were interested in zero-angular-momentum states. These can be constructed with great accuracy out of basis states in which the angular momentum between any two particles as well as that between the center of mass of these two and the third particle is zero.

We compare the results of the ACCC method with those of the CSM. The three-body bound-state problem was solved by the stochastic variational method [18]. The ACCC and CSM trajectories obtained by varying λ are shown in Fig. 4 for $B=0$ and $B=1$ MeV. The two methods give the same pole positions for a wide range of the potential strength. The branching-off point is (close to) the origin, irrespective of whether the potential has a barrier or not. Thus the behavior of the Borromean system for the S wave is similar to a two-body case with finite barrier. This is consistent with the well-known interpretation that the three-body system has an effective barrier against disintegration even for zero orbital angular momentum.

B. Application to the resonances in ^{9}Be and ^{9}B

The $\alpha+\alpha+N$ type microscopic three-cluster model we use for ^{9}Be and ^{9}B is a straightforward extension of the $\alpha+N$ model used in Sec. II C for ^{5}He and ^{5}Li. The model has been detailed in Ref. [11], where it has been shown to reproduce a number of properties of ^{9}Be and ^{9}B successfully. The trial wave function is chosen as

$$\Psi=\sum_{\mu}\sum_{l_1,l_2,L}\mathcal{A}\{\Phi_{\alpha_1}\Phi_{\alpha_2}F^{\mu}_{l_1l_2L}(r_1^{\mu},r_2^{\mu}) \times[[Y_{l_1}(\hat{\mathbf{r}}_1^{\mu})\times Y_{l_2}(\hat{\mathbf{r}}_2^{\mu})]_L\times\chi_{1/2}]_{JM}\}, \tag{10}$$

where μ stands for either of the two cluster arrangements $(\alpha N)\alpha$ and $(\alpha\alpha)N$, and $\mathbf{r}_1^{\mu}$ and $\mathbf{r}_2^{\mu}$ denote the Jacobi coordinates belonging to the arrangement μ. The variable functions $F^{\mu}_{l_1l_2L}(r_1^{\mu},r_2^{\mu})$ are constructed by expansions in terms of Gaussians. In Ref. [11] the resonances were treated by the CSM, and they showed good correspondence with experiment. The only exception is that the CSM was unable to

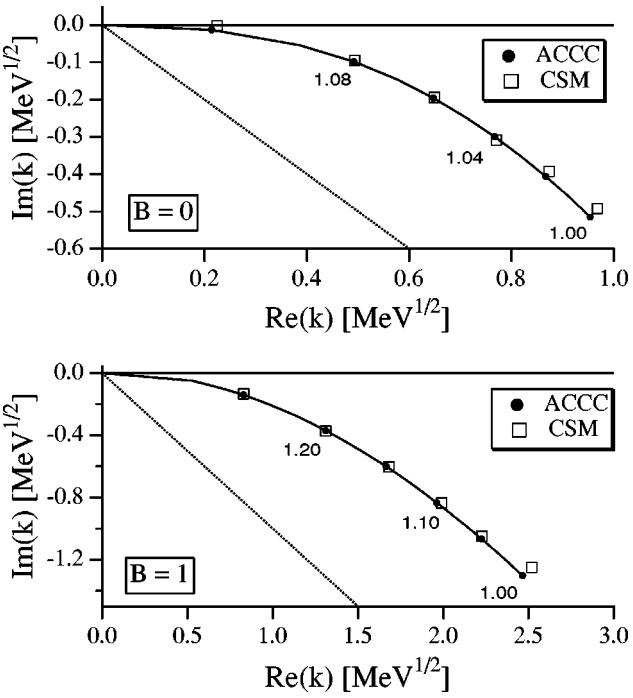

FIG. 4. The trajectories of the resonance of a Borromean system interacting via the two-range Gaussian potential of Eq. (11). The value B, given in MeV, denotes the strength of the repulsive part. The ACCC trajectory as a function of the coupling constant λ is compared with the CSM result. Here k is identified with $E^{1/2}$.

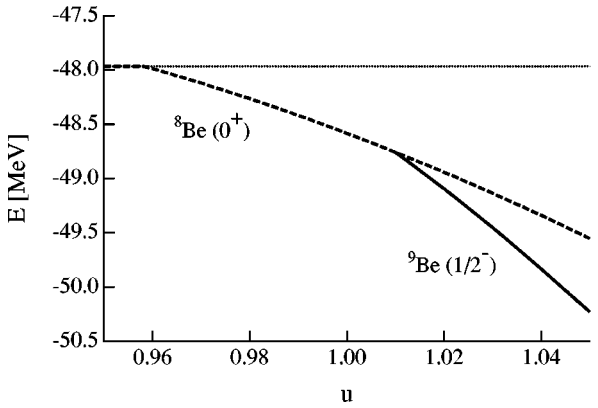

FIG. 5. The energy of the $1/2^-$ state of ^{9}Be as a function of the u parameter. The energy of the subsystem ^{8}Be is also shown.

produce a $1/2^+$ resonance, which was identified experimentally near threshold for both nuclei. In the microscopic $\alpha+\alpha+N$ model, the Minnesota force was adopted.

The coupling constant λ has again been chosen to be proportional to u. The appropriate u value recommended in the literature is around 0.94; this makes ^{8}Be in the consistent $\alpha+\alpha$ model slightly unbound as it should be, and both ^{5}He and ^{5}Li are also unbound. As was mentioned in Sec. II C, the energy of the α particle is unaffected by the value of u, but since both the $\alpha+\alpha$ and the $\alpha+N$ energies depend on u, the two-body thresholds do also depend on u. Both ^{9}Be and ^{9}B are Borromean, and so in the neighborhood of $\bar{u}$ the lowest-lying threshold is the three-body threshold, but that is not the case for larger u values that make the three-cluster states of our interest bound. In the procedure of analytic continuation this requires subtle considerations.

Figure 5 displays the bound-state energy of the $1/2^-$ state in ^{9}Be as a function of u. The energy of the corresponding $\alpha+\alpha$ model of ^{8}Be is also shown. The calculated value of the intrinsic α-particle energy is -23.984 MeV (the Coulomb potential is included); so ^{8}Be gets bound if the energy is deeper than -47.968 MeV, which occurs for $u \geqslant 0.958$. In the $J^\pi = 1/2^-$ state the $\alpha+\alpha+n$ system is more deeply bound than the $\alpha+\alpha$ system for $u > 1.01$. Therefore, the $1/2^-$ state will be unstable to the dissociation into the ^{8}Be $+n$ channel for $u \leqslant 1.01$. The analytic continuation is to be based on bound states, and the quantity to be continued is the square root of the energy with respect to the threshold reached first from below for decreasing u. The first threshold one reaches by decreasing u is the ^{8}Be$+N$ threshold for all cases to be considered. Thus, what we have to continue analytically is $k(u) = \sqrt{E(^9\mathrm{Be}) - E(^8\mathrm{Be})}$. The resonance energy obtained is then, of course, that with respect to the energy of ^{8}Be. The energy $E(^8\mathrm{Be})$ is complex in the u region in which

TABLE II. Energies E and widths Γ, given in units of MeV, of ^{8}Be, ^{9}Be, and ^{9}B. $\bar{u} = 0.94$. The energy of ^{8}Be is counted from the two-body threshold and the energies of ^{9}Be and ^{9}B from the three-body threshold.

		ACCC		CSM [a]		Expt. [b]	
	J^π	E	Γ	E	Γ	E	Γ
^{8}Be	0^+	0.208	0.003			0.09189	6.8 ± 1.7 eV
	2^+	2.85	1.44			3.132 ± 0.03	1.5 ± 0.02
^{9}Be	$3/2^-$	-1.501	0	-1.431	0	-1.5735	0
	$5/2^-$	0.838	0.001	0.84	0.001	0.8559 ± 1.3	0.77 ± 0.15 keV
	$1/2^-$	1.17	0.59	1.20	0.46	1.21 ± 0.12	1.080 ± 0.11
^{9}B	$3/2^-$	0.288	0.001	0.30	0.004	0.277	0.54 ± 0.21 keV
	$5/2^-$	2.56	0.05	2.55	0.044	2.638 ± 0.005	0.081 ± 0.005
	$1/2^-$	2.66	1.15	2.73	1.0	3.11[c]	3.1

[a]Reference [11].
[b]Reference [12].
[c]B. Pugh, quoted in Ref. [33].

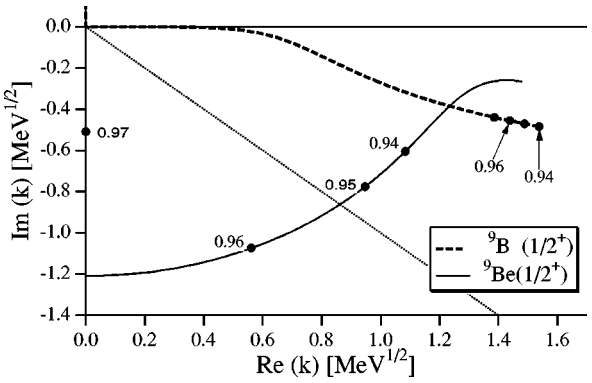

FIG. 6. The trajectories of the $1/2^+$ states in ^{9}Be and ^{9}B as a function of the u parameter. Here k is identified with $E^{1/2}$. The dotted line marks Im $k=-$Rek.

$\alpha+\alpha$ is unbound, i.e., for $u<0.958$.

The resonance parameters obtained for the $1/2^-$, $3/2^-$, and $5/2^-$ states of ^{9}Be and ^{9}B are compared in Table II with experiment and with the previous CSM calculation of [11]. The agreement between the ACCC and CSM results is very good, and the theory reproduces the measured resonance energies remarkably well. The resonance widths are reasonably well reproduced. The basis dimension used in the present calculation is much larger than that used in Ref. [12], and that is why the ^{9}Be ground state has a slightly larger binding energy now.

The results of the analytic continuation for the $1/2^+$ states of ^{9}Be and ^{9}B are shown in Fig. 6. The ^{9}Be trajectory shows the typical behavior of an S-wave two-body state with an attractive potential. It is certainly different from the pattern of Fig. 4 expected for a Borromean system. The virtual-state section is easily understood by recalling that, from the origin to the point marked with $u=0.96$ (more precisely, $u=0.958$), the model subsystem $\alpha+\alpha$ is indeed bound. But the behavior of the curve is similar even beyond that point, which indicates that this state is indeed of the ^{8}Be$+n$ structure. The point corresponding to the physically correct potential ($\bar{u}=0.94$) is in the region of physical resonances, but is still close to the borderline of the unphysical region. The ^{9}B trajectory is, on the other hand, reminiscent of either a two-body resonance with a barrier, like the $B\neq 0$ case of Fig. 2, or of a true three-body resonance of a Borromean system, shown in Fig. 4. It is obvious that, owing to the higher Coulomb barrier and the sharp resonance in the $\alpha+\alpha$ system, the $\alpha-\alpha$ subsystem tends to be formed more dominantly than the $\alpha+p$ subsystem, but the trajectory alone cannot tell us whether the weight of the ^{8}Be$+p$ configuration is large enough to prevail over the $\alpha+\alpha+p$ three-body structure. In comparing the motion of the two poles, it is conspicuous that the rate of change of $k(u)$ along the trajectory is much larger for ^{9}Be than for ^{9}B.

Table III contains the resonance parameters of the $1/2^+$ states in ^{9}Be and ^{9}B. As they depend rather strongly on the u value, which is poorly defined, they are presented for a range of u values. Furthermore, to help decide between the different u values, parallel results for ^{8}Be and for the $5/2^+$ state of ^{9}Be are also shown. From this it appears that, rather than 0.94, the appropriate value is 0.95; for $\bar{u}=0.95$, all resonance energies are reasonably well reproduced. But the widths for the $1/2^+$ states of ^{9}Be and ^{9}B are much larger than the empirical values. It is difficult to reconcile the theoretical result with experiment in this respect. The three-cluster dynamics is described very accurately in our model and any excitation mechanism that would invalidate the model should show up in either $\alpha+\alpha$ or $\alpha+N$, but there seems to be no such effect. A stringent test of the correctness of our results would be a comparison with experimental data other than resonance parameters. For example, the rate of the $1/2^+\rightarrow 3/2^-$ transition, which is known experimentally [12], could be calculated by an analytic continuation of the corresponding matrix elment.

In a recent preprint [34] Efros and Bang have concluded that the $1/2^+$ state of ^{9}Be is a virtual state with an energy of -23.5 keV, and in their model this implies that the analog state in ^{9}B is a resonance of width 1.5 MeV at 0.6 MeV. They described ^{9}Be in a macroscopic $\alpha+\alpha+n$ model and analyzed the photodisintegration of ^{9}Be, assuming a ^{8}Be $+n$ two-body final state. The interaction between ^{8}Be and n was represented by a two-body potential, and the $1/2^+$ states were produced as states in this potential. While it is obvious that our microscopic three-cluster model, in principle, is far more realistic than a macroscopic two-body potential model, this two-body model has the advantage that its parameters carry direct empirical information. It is therefore worthwhile to ponder the relationship between the two results. As is shown in Table III, our model would put the ^{9}Be $1/2^+$ state at -0.0235 MeV with a u value slightly larger than 0.97. The same u value would put the $1/2^+$ resonance of ^{9}B at 1.5

TABLE III. Resonance energies E and widths Γ, given in units of MeV, of the $1/2^+$ states of ^{9}Be and ^{9}B. The energy is counted from the three-body threshold.

	^{9}Be($1/2^+$)		^{9}B($1/2^+$)		^{8}Be(0^+)		^{9}Be($5/2^+$)	
$\bar{u}$	E	Γ	E	Γ	E	Γ	E	Γ
0.94	1.02	2.62	2.3	2.7	0.208	0.0026	2.06	0.60
0.95	0.40	2.94	2.1	2.6	0.101	20 eV	1.86	0.52
0.96	-0.84	2.41	1.86	2.4	-0.020 [b]	1.65	0.45	
0.97	-0.26 [c]	1.62	2.2	-0.153 [b]	1.42	0.37		
Expt. [a]	0.111 ± 0.007	0.217 ± 0.010	(1.9)	~ 0.7	0.09189	6.8 ± 1.7 eV	1.476 ± 0.009	0.282 ± 0.011

[a]Reference [12].
[b]Bound state.
[c]Virtual state.

MeV and a width of 2 MeV. This minor inconsistency with the prediction of the two-body model is attributed to the two-body dynamics in that model. The same u value would make ^{8}Be bound, which is incorrect, but it would shift the $5/2^+$ state of ^{9}Be close to (but slightly below) its correct position. This shows that u depends slightly not only on the nucleus but also on the state, and if so, $u>0.97$ cannot completely be ruled out for the $1/2^+$ state of the $\alpha+\alpha+N$ system. Thus our model does not exclude that the $1/2^+$ state of ^{9}Be is actually a virtual state. If $u>0.97$ were appropriate for the $1/2^+$ state of the $\alpha+\alpha+N$ system, then a further fine-tuning of the force would be desirable so as to make ^{8}Be unbound since the binding of ^{8}Be distorts the dynamics of the $\alpha+\alpha+N$ systems.

IV. CONCLUSION

In this paper we have located unbound states by analytic continuation of the momentum as a function of a potential strength from the bound-state region (using the ACCC method). The objective was to study controversial unbound states of the most typical two-cluster and three-cluster nuclei. In this way we tested the applicability of the analytic continuation method, and explored the nature of the states considered. We found some general results and some that are pertinent to the systems investigated.

The general results are the following. First, we were particularly interested in $l=0$ states, where the branching-off of the pole trajectory from the imaginary k axis is at an *a priori* unknown point of the negative imaginary k axis. We have demonstrated that a linear extrapolation of the momentum in the vicinity of the branching-off point performs excellently for $l=0$ states as well. This makes it possible to locate any $l=0$ unbound states: virtual states, unphysical resonances, or resonances. Second, we have demonstrated that the three-body resonances of Borromean systems that interact via purely attractive forces behave like two-body resonances within a potential barrier. In this way we confirmed the appearance of an effective three-body barrier. Third, we have demonstrated that the analytic continuation is feasible and reliable even if the two-body thresholds, as functions of the coupling constant, cross the three-body threshold. This is a significant finding because it extends the scope of the method. In fact, in an n-body system ($n>2$) there may be no parameter whose change varies the n-body binding but leaves the $n-1,n-2,\ldots$ binding energies intact. This implies that a variation of any coupling constant will rearrange the binding mechanism, but our result shows that the true natures of the unbound states can still be explored by analytic continuation.

Turning to more specific results, we mention that several comparisons were made between the ACCC method and the CSM and a scattering-wave method. Whenever results obtained with these other methods are available, good agreement has been found, which is a confirmation of the validity of all these methods. In particular, the position of the $1/2^-$ resonance of the $\alpha+N$ system has been confirmed to be much lower than obtained in conventional phenomenological analyses. This is not a discrepancy between theory and experiment but rather a failure of the conventional R-matrix parametrization.

There are cases in which no resonances have been found with any other method, despite physical indications for their existence. With the ACCC method the poles have been successfully located even in these cases. Their absence in the CSM is now understood and discussed by the close vicinity of the unphysical region in the k plane. The borderline is given by $\mathrm{Im}\,k=-\mathrm{Re}k$ or by the k phase $-\pi/4$. To find poles with such phases by the CSM requires a rotation angle $\theta \approx \pi/4$, with which the CSM is bound to become very unstable. For the $1/2^+$ states of ^{5}He and ^{5}Li, the long-standing contradiction [22] between bound-state and unbound-state methods is now resolved. The latter failed to find these $1/2^+$ states because they lie very far from where they were predicted to be by bound-state methods, at the borderline of the unphysical resonance region. There can be no doubt in the correctness of the cluster-model predictions since the S-wave phase shifts are excellently reproduced. The fact that bound-state methods incorrectly predict the $1/2^+$ states to be so low in energy is a warning that one should not take quite seriously the correspondence between the energies of states found in the shell model or any other method and the energies of unbound states. At the same time, this warning should be taken as a stimulation to use them in analytically continued form; after all, there is no essential difference between the cluster model and the shell model in this respect.

The preeminence of the ACCC method becomes apparent for three-body resonances, for which scattering-state methods are useless and the CSM is unstable. The $1/2^+$ states of ^{9}Be and ^{9}B have been found. From the pole trajectories it is apparent that a $^8\mathrm{Be}+N$ structure is more prominent in ^{9}Be than in ^{9}B. In comparing the results with experiment, one should keep in mind that the widths of the resonant states change together with their positions (as functions of any parameter of the model), and they change very rapidly below the Coulomb barrier. In view of this, the agreement with experiment is very satisfactory apart from the widths of the $1/2^+$ states.

In conclusion, we can state that the ACCC method has been found to be unique among the techniques of localizing unbound states of composite systems. It performs uniformly well, irrespective of the decay mode and of the location of the unbound state in the complex k plane. It has proved to be a useful theoretical tool that broadens the scope of conventional nuclear structure models by incorporating the unbound-state region of the nuclear spectrum.

ACKNOWLEDGMENTS

We are grateful to Dr. F. Coester for his careful reading of the manuscript. This work was supported by Grants-in-Aid for Scientific Research (No. 10640255) and for International Scientific Research (Joint Research) (No. 08044065) of the Ministry of Education, Science and Culture (Japan) and by the OTKA Grant No. T17298 (Hungary). As part of the intergovernmental scientific and technological cooperation between Hungary and Japan, it has been supported by OMFB, Hungary, and the Science and Technology Agency, Japan.

[1] V. I. Kukulin, V. M. Krasnopol'sky, and J. Horáček, *Theory of Resonances: Principles and Applications* (Kluwer Academic, Dordrecht, Netherlands, 1989), p. 219
[2] M. V. Zhukov, B. V. Danilin, D. V. Fedorov, J. M. Bang, I. J. Thompson, and J. S. Vaagen, Phys. Rep. **231**, 150 (1993).
[3] R. G. Newton, *Scattering Theory of Waves and Particles* (Springer, Berlin, 1982), p. 357.
[4] A. G. Sitenko, *Scattering Theory*, Springer Series in Nuclear and Particle Physics (Springer, Berlin, 1991), p. 100.
[5] B. G. Giraud, M. V. Mihailović, R. G. Lovas, and M. A. Nagarajan, Ann. Phys. (N.Y.) **140**, 29 (1982).
[6] A. Csótó, R. G. Lovas, and A. T. Kruppa, Phys. Rev. Lett. **70**, 1389 (1993).
[7] A. U. Hazi and H. S. Taylor, Phys. Rev. A **1**, 1109 (1970).
[8] Y. K. Ho, Phys. Rep. **99**, 1 (1983).
[9] V. I. Kukulin and V. M. Krasnopol'sky, J. Phys. A **10**, 33 (1977); V. I. Kukulin, V. M. Krasnopol'sky, and M. Miselkhi, Sov. J. Nucl. Phys. **29**, 421 (1979).
[10] N. Tanaka, Y. Suzuki, and K. Varga, Phys. Rev. C **56**, 562 (1997).
[11] K. Arai, Y. Ogawa, Y. Suzuki, and K. Varga, Phys. Rev. C **54**, 132 (1996).
[12] F. Ajzenberg-Selove, Nucl. Phys. **A490**, 1 (1988).
[13] M. A. Tiede *et al.*, Phys. Rev. C **52**, 1315 (1995).
[14] F. C. Barker, Phys. Rev. C **53**, 2539 (1996).
[15] R. Sherr and G. Bertsch, Phys. Rev. C **32**, 1809 (1985).
[16] H. M. Nussenzweig, Nucl. Phys. **11**, 499 (1959); *Causality and Dispersion Relations* (Academic Press, New York, 1972), p. 221.
[17] V. I. Kukulin and V. M. Krasnopol'sky, J. Phys. G **3**, 795 (1977).
[18] K. Varga and Y. Suzuki, Phys. Rev. C **52**, 2885 (1995).
[19] T. Vertse, K. F. Pál, and Z. Balogh, Comput. Phys. Commun. **27**, 309 (1982).
[20] C. L. Woods, F. C. Barker, W. N. Catford, L. K. Fifield, and N. A. Orr, Aust. J. Phys. **41**, 525 (1988).
[21] A. Csótó and G. M. Hale, Phys. Rev. C **55**, 536 (1997).
[22] A. Csótó and R. G. Lovas, Phys. Rev. C **53**, 1444 (1996).
[23] P. Navrátil and B. R. Barrett, Phys. Rev. C **54**, 2986 (1996).
[24] D. R. Thompson, M. LeMere, and Y. C. Tang, Nucl. Phys. **A286**, 53 (1977); I. Reichsten and Y. C. Tang, *ibid.* **A158**, 529 (1970).
[25] G. M. Hale, R. E. Brown, and N. Jarmie, Phys. Rev. Lett. **59**, 763 (1987).
[26] R. G. Lovas, K. Arai, Y. Suzuki, and K. Varga, Nuovo Cimento A **110**, 907 (1997).
[27] V. B. Belyaev and K. Möller, Z. Phys. A **279**, 47 (1976).
[28] W. Glöckle, Phys. Rev. C **18**, 564 (1978).
[29] A. Matsuyama and K. Yazaki, Nucl. Phys. **A534**, 620 (1991).
[30] A. Csótó, H. Oberhummer, and R. Pichler, Phys. Rev. C **53**, 1589 (1994).
[31] Y. Suzuki and K. Varga, in *Stochastic Variational Approach to Quantum-Mechanical Few-Body Problems*, Lecture Notes in Physics, Vol. m54 (Springer, Berlin, 1988).
[32] V. Efimov, Phys. Lett. **33B**, 563 (1970).
[33] M. A. Tiede *et al.*, Phys. Rev. C **52**, 1315 (1995).
[34] V. D. Efros and J. M. Bang, Eur. Phys. J. A (to be published).